ARTICLE NO. 80-4078

Chain Reaction cw HF Laser with Stationary Shock Initiation

James P. Moran,* Alan C. Stanton,† and R. Bruce Doak‡
Aerodyne Research Inc., Bedford, Mass.

A new kind of chain reaction cw HF laser, initiated by atomic fluorine produced in the reaction $NO+F_2 \rightarrow FNO+F$, has been developed. Uniform premixing of the reactant gases is achieved with negligible reactions in a cold supersonic stream, and combustion is initiated by a nearly-normal stationary shock. This work represents the first reported demonstration of cw chemical laser action by stationary shock initiation. A small blowdown shock holder system was constructed to study the shock initiation laser scheme. A closed cavity stable resonator laser configuration was used in the shock holder, and HF laser action was confirmed by measurements of the IR cavity intensity and by mirror calorimetry. Optimum performance was achieved in a mixture of 13.7% F_2, 2.7%H_2, 5.4% NO, in helium diluent, with a shock holder pressure of 13 Torr. The optical axis (mirror co-normal) was located approximately 3.3 cm downstream from the normal shock. A total out-coupled energy of 41 J over a lasing duration of 0.75 s was measured, corresponding to 55 W average power. A lasing zone at least 3.4 cm in length was indicated, with peak cavity intensity of approximately 100 W/cm^2. The chemical efficiency for these conditions was conservatively estimated to be 1%.

Introduction

A new kind of cw HF chain reaction laser is reported here. The chain reaction is initiated by atomic fluorine produced by the reaction $NO+F_2 \rightarrow FNO+F$. The temperature-dependent rate for this reaction was measured by Kolb[1] in an earlier phase of this study. For cw laser operation, uniform premixing of the reactant gases is achieved in a cold supersonic stream with negligible reactions, and combustion is initiated by a nearly normal stationary shock. This work represents the first reported demonstration of cw chemical laser action by stationary shock initiation.

Chemically pumped laser radiation has been induced by a traveling detonation wave, as first reported by Gross et al.[2] in shock tube studies with mixtures of F_2O, H_2, and Ar. Stationary shock waves have been achieved in premixed detonable gases in various flow configurations by several investigators. The feasibility of achieving continuous wave laser radiation from a purely chemically pumped H_2+Cl_2 system, in which chemical reactions are initiated in a premixed stream by a stationary shock wave, was examined theoretically by Bowen and Overholser.[3] In their studies, the chain reaction was postulated to be initiated by thermal dissociation of Cl_2. They concluded that the scheme might be pursued with a reasonable expectation of success. This scheme has not been demonstrated experimentally, however. In HF/DF laser systems, atomic fluorine production may be achieved with little chemical heat release by the reaction of nitric oxide with molecular fluorine. This mechanism was used successfully by Cool et al.[4] in an HF chemical diffusion laser, but has not previously been considered in a fully premixed cw laser application.

Complex nonequilibrium processes in highly exothermic gas phase reactions may be studied most easily in steady flow. Stationary shock initiation of reactions offers a convenient configuration for such studies, since thorough gas mixing may be achieved in the cold supersonic flow upstream from the shock wave. In detonable§ mixtures, one has limited options in flow geometries, since the stationary shock must be isolated from the wall boundary layers of the supersonic mixing zone. Three shock configurations have previously been demonstrated: 1) a Mach-disk shock formed by the convergence of the barrel shock in a highly underexpanded supersonic jet[5-7]; 2) the normal shock produced by Mach reflection of two converging oblique shocks, which emanate from facing wedges in a supersonic wind tunnel[8,9]; and 3) the normal shock produced in an overexpanded two-dimensional jet in which boundary suction was applied at the end of the supersonic mixing section.[10] In all of these studies, the initiating shock was isolated from the boundary layers of the mixing section. All studies were conducted with preheated air in the main supersonic stream and fuel injection through a single axisymmetric or linear injector, so that only a central portion of the supersonic stream was uniformly premixed. This configuration allowed area relief downstream from the initiating shock to prevent flow choking. These techniques provide a stationary reference frame for studies of chemical kinetics; however, they are not suitable for the present application of stationary shock initiation of continuous wave lasers.

In this paper, a new shock holder configuration is described which is more suitable for cw laser applications. Specifically, one requires efficient gas usage and high pressure recovery. When premixing is achieved in a supersonic stream, one would hope to recover a major portion of the flow at a pressure which is large relative to that in the supersonic stream. In the stationary shock configuration of Nicholls et al.[5-7] the highly underexpanded jet precludes efficient pressure recovery. In the converging flow geometry of Gross[8] and Richmond and Shreeve[9] a premixed detonable mixture may exist in only a small central portion of the supersonic stream to avoid choking, thus precluding efficient gas usage. The overexpanded jet configuration of Suttrop[10] allows flow expansion downstream from the normal shock; consequently, the degree of gas usage may be limited only by the fraction of

Received May 26, 1978; revision received Feb. 4, 1980.

Index categories: Lasers; Shock Waves and Detonations.

*Principal Research Scientist; presently with Avco Everett Research Laboratory, Inc., Everett, Mass.

†Senior Research Scientist.

‡Research Scientist; presently with Max Planck Institute, Goettingen, West Germany.

§Detonable here implies that no stationary flow is possible if reactions go to completion at constant area. Flow choking would cause upstream propagation of the initiating shock.

the jet flow which crosses the normal shock. Pressure recovery is limited mainly by the extent to which the jet flow may be overexpanded and, hence, by the extent of wall boundary layers. The results reported by Suttrop show a ratio of postshock recovery pressure to supersonic static pressure of 2.82. The shock holder reported here achieves pressure recovery ratios typically greater than 7 for more than 68% of the total supersonic flow.

In the present system, a premixed detonable mixture is directed into a chamber as a slightly underexpanded free jet. This supersonic jet is interrupted shortly downstream from the exit by a nearly normal shock wave. The shock is held in a stationary manner by a shock holder which accepts only a portion of the total jet flow. An adjustable sonic throat within the shock holder controls the accepted fraction. Any fraction less than that appropriate for supersonic entry forces the occurrence of a normal shock slightly upstream from the shock holder inlet. Shock standoff distance is coupled to accepted fraction, and backpressure in the free jet chamber is controlled by the rejected flow fraction and blowdown receiver geometry.

Experimental Appparatus

Major system components are shown in the assembly in Fig. 1. The diluent (He or Ar) enters the rear of the primary plenum which is rectangular in cross section with inner dimensions of 4.0 cm height and 10.0 cm in width. Diluent flow is divided as a core flow and a shroud flow. These flows are separated by a thin-walled conduit of rectangular cross section with dimensions of 2.0 cm in height and 8.0 cm in width. The heights of the plenum and core flow conduits taper proportionately to 2.0 and 1.0 cm, respectively, at the inlet to the nozzle array. Fluorine is injected through 11 holes equally spaced across the core in each of two tubes which traverse the plenum at positions approximately 30 cm upstream from the nozzle inlet plane. The shroud flow, which does not contain reactive gases, serves to isolate the walls of the supersonic-mixing region and the upstream portion of the shock holder and thereby prevents wall-induced reactions.

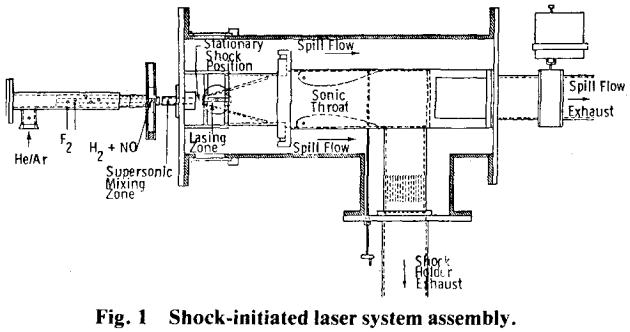

Fig. 1 Shock-initiated laser system assembly.

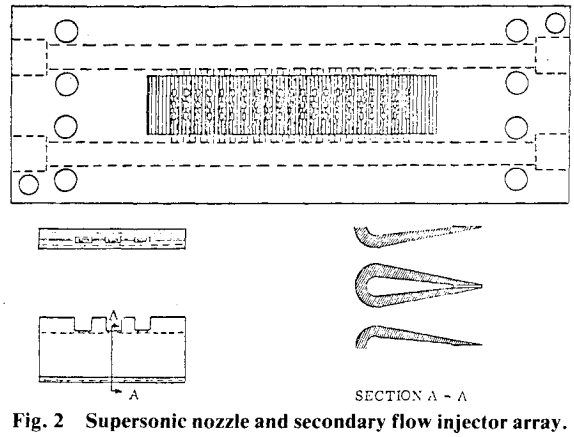

Fig. 2 Supersonic nozzle and secondary flow injector array.

The 25-element nozzle array was fabricated from a single piece of beryllium copper and is shown in an upstream view in Fig. 2. The two-dimensional nozzle elements have a throat height of 1.27 mm with 4.06 mm spacing on centers and 0.25 mm trailing edge thickness. Converging nozzle walls are circular arcs, and diverging walls are straight with a divergence half angle of 9.4 deg. Secondary flow, consisting of hydrogen and nitric oxide, enters a manifold through four holes in the sides of the nozzle block. Secondary injection occurs through three slits along each trailing edge of the central 21 nozzle elements, as shown in three views of a single nozzle wall element in Fig. 2. Overall dimensions of the nozzle array are 2.0 cm in height and 10.0 cm in width. Secondary injection is confined to the central 1.0 cm in height and 8.0 cm in width which coincides with the fluorine bearing core flow.

The supersonic mixing section, shown in Fig. 1, is rectangular in cross section and slightly divergent, increasing from 2.0 to 3.05 cm in height and from 10.0 to 11.2 cm in width over a length of 24.0 cm. The exit plane of the mixing section extends 2.54 cm into a cylindrical chamber (spill flow chamber) which is 38.0 cm in diameter.

The shock holder is shown within the spill flow chamber in Fig. 1. Mirrors which are 10.0 cm in diameter form the sidewalls of the shock holder inlet. One mirror is concave spherical with a radius of 5.0 m; the other is flat. Machined mirror edges form two sides of a sharp, rectangular entrance which is positioned 2.54 cm downstream from the exit of the supersonic mixing section. Copper or Lexan plates form the other two walls, which have a slight divergence to prevent choking of the flow as the chemical reactions progress. Inlet widths of 11.2 and 10 cm and inlet heights of 2.51 and 2.11 cm were used for work reported herein.

The position of the stationary normal shock between mixing section exit and shock holder entry is controlled by a sonic throat of variable height, shown in Fig. 1. In normal operation, flow is first established without reactions, then fluorine is introduced and the resultant reactions cause the flow to re-establish itself with the desired shock position. The sonic throat area is chosen to produce an internal shock pattern near the shock holder inlet in the absence of reactions. As reactions proceed downstream from this shock pattern, resultant rise in temperature prevents full flow acceptance by the fixed sonic throat. Consequently, the shock pattern is driven slightly upstream from the shock holder inlet and assumes a nearly normal configuration. High pressure recovery and nearly stagnation temperature are achieved at the shock holder inlet. These conditions are appropriate to initiate the desired reactions for a chemical laser.

Downstream of the sonic throat, the shock holder flow is conveyed through cooling fins to a dump tank with a volume of 2.78 m^3. The portion of flow which spills over the shock holder inlet exhausts to a separate dump tank with a volume of 5.57 m^3. This flow originates primarily from the shroud flow; consequently, it should experience little temperature rise due to reactions. The run duration (typically 0.7-1.2 s) for this blowdown system is controlled by spill flow.

Fluid Flow Instrumentation and Control

Chemical composition is determined from measured flow rates of the various constituents using calibrated metering

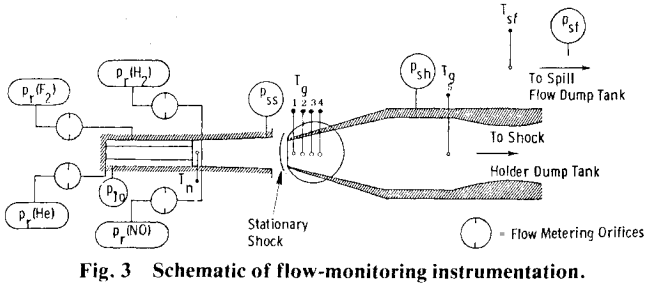

Fig. 3 Schematic of flow-monitoring instrumentation.

orifices. Pressures in supply reservoirs are recorded on a single channel of an oscillograph through a scanner which samples each of four pressure transducers at 0.05-s intervals. A schematic of flow-monitoring temperature and pressure instrumentation is shown in Fig. 3. Four oscillograph channels continuously record transducer measurements of primary plenum pressure, static pressure at a station 0.635 cm upstream from the exit of the supersonic throat, and stagnation pressure in the spill flow chamber. Nozzle temperature is sensed with a chromel/alumel thermocouple. Center-stream gas temperature at four stations within the laser cavity and at one station located 33 cm downstream from the shock holder inlet are sensed with platinum/platinum-13% rhodium thermocouples which are sheathed in inconel (sheath outer diameter = 0.20 mm). Signals from these six thermocouples plus signals from four mirror thermocouples are recorded on a single oscillograph channel through a scanner which samples each of the ten thermocouple signals at 0.1-s intervals.

Before each run, the dump tanks and test chamber are evacuated to a pressure below 0.1 Torr, and the dump tanks are isolated from the system by a solenoid-controlled helium-driven ball valve. Valve and recorder operations are controlled by sequentially-triggered variable time-delay relays.

Shock position and shape were observed with a Schlieren system which views the region between the exit of the supersonic mixing section and the entrance to the shock holder. The system employs an arc lamp, 48.4-cm focal length lenses and a 16 mm motion picture camera which operates at 64 frames/s.

Laser Instrumentation

The performance of the shock-initiated laser is monitored through measurements of mirror heating and gas heating and through infrared radiation measurements of the cavity intensity. For the mirror calorimetry measurements, the cavity mirrors (10.0-cm diam × 6.35-mm thickness) are each instrumented with a thermistor and with embedded chromel/alumel thermocouples. The mirror thermocouples are paired in series; each pair consists of one thermocouple from each mirror at the same streamwise station. The thermistor signal provides a sensitive measurement of the mirror temperature rise after temperature uniformity is achieved and thus provides an indication of the total energy input to the mirrors due to lasing and chemical reactions. The thermocouples provide a redundant measurement of the total energy input and, in addition, they respond to local heating due to lasing during the course of the run. With amplification, the oscillograph response to the mirror thermocouples is 0.58°C/cm, and the response to the thermistor signal is 0.13°C/cm.

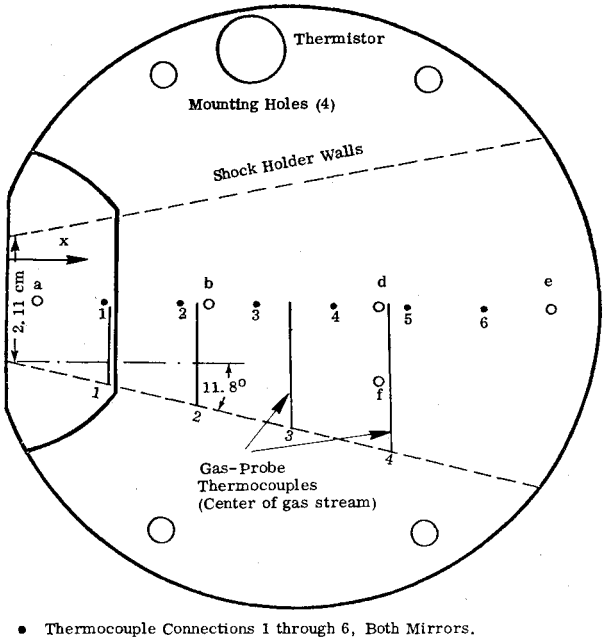

• Thermocouple Connections 1 through 6, Both Mirrors.
o Cavity Sampling Holes a through e (0.75 mm diam.) Flat Mirror.

Fig. 4 Laser performance instrumentation, configuration A.

The configuration of the mirror thermocouples and thermistors in relation to the mirror and shock holder geometry is indicated in Fig. 4. The positions of the four gas probe thermocouples, which are located in the laser cavity region, are also indicated in this figure. The thermocouple locations are given in Table 1. The gas probe thermocouples, discussed in the previous section, were used to monitor the gas heating due to chemistry. These thermocouples also responded consistently to local laser heating in regions of high cavity intensity, and, thus, were useful as laser performance indicators. Also shown in Fig. 4 are cavity radiation sampling holes in the flat mirror which were used in the cavity intensity measurements described below (locations are given in Table 1). The overall configuration in Fig. 4, designated configuration A, was used for most of the experiments discussed in this paper.

A second laser instrumentation arrangement, using a different mirror pair, was used in obtaining finer detail in cavity radiation measurements. In this configuration, designated configuration B, the spherical mirror was again instrumented with a thermistor and six chromel/alumel thermocouples as indicated in Fig. 4 and Table 1. Additional cavity radiation sampling holes were included in the flat mirror in configuration B, as shown in Table 1, and mirror thermocouples 3 and 4 on that mirror were eliminated.

The measurements of laser cavity intensity were made with an array of three room temperature lead selenide detectors (2 × 2 mm) which viewed the laser radiation emitted through the cavity sampling holes in the flat mirror through a CaF_2 window. The locations of the radiation sampling holes are indicated in Table 1 for the two configurations used in the experiments. Small diffracting apertures (70 μm diam in configuration A and 35 μm diameter in configuration B) were mounted and centered behind 0.75-mm-diameter holes in the flat mirror. The PbSe detector elements were mounted on an oscillating arm which swept the detector array across the diffraction patterns of the small apertures at frequencies of 4 or 8 Hz. The detectors were mounted in a line perpendicular to the sweep plane with the middle detector centered on the diffraction peaks. Additional masking apertures were

Table 1 Locations of the mirror and gas probe thermocouples and cavity sampling holes relative to the shock holder inlet

Mirror thermocouple	x,cm	Gas probe thermocouple	x,cm
1	1.54	1	1.66
2	2.81	2	3.22
3	4.08	3	4.78
4	5.35	4	6.35
5	6.62	5	33.0
6	7.89		
Config. A	**x,cm**	**Config. B**	**x,cm**
hole		hole	
	0.424	a	0.424
b	3.28	b	1.85
d	6.14	d	3.28
e	9.00	e	4.23
		f	5.19
		g	6.14
		h	7.57
		i	8.00

positioned 5.77 cm from the mirror holes so that the on-axis diffracted radiation from the various mirror sampling stations would be separated in the plane of the detectors. The radiation pattern, in the detector plane, thus consists of the projections of the masking apertures. These projections are separated circles of 0.81-cm diameter. As the 2×2 mm PbSe detector sweeps across this pattern, it is sequentially exposed to the on-axis diffracted radiation from each of the cavity sampling holes. Broad angular diffraction in this arrangement allows the measured absolute power incident on the detectors to be related to the laser cavity intensity at each sampling location with minimal requirements in alignment precision.

The absolute responsivity of the PbSe detectors was measured using a black-body radiation source at 920 K, which consisted of a resistively heated graphite rod with a hollowed uniform-temperature cavity. The cavity was viewed by the detector through a 0.56-cm-diam hole. The source cavity temperature was measured with a platinum/platinum-13% rhodium thermocouple. Emerging radiation was focused onto the detector array with an infrared-transmitting lens through a wide bandpass filter (2.2-4.2 μm). The product of blackbody spectral radiation, measured lens and filter spectral transmissions, and detector relative spectral response was integrated over the filter bandpass to provide a direct relationship between detector signal and absolute detector responsivity at 2.8 μm. The electronics data train was identical to that employed in the laser radiation measurements, thus providing a direct calibration of oscillograph deflections. The result of this calibration was in good agreement with the manufacturer's stated detector responsivity. The oscillograph response at unity amplifier gain to the measurements of cavity radiation intensity was 1.02×10^2 W/cm^2/cm deflection using the 70-μm diffracting holes and 1.63×10^3 W/cm^2/cm deflection using the 35-μm holes. Specified hole sizes were verified by observing the visible diffraction of a He-Ne laser beam passed through the holes.

The optical alignment of the laser cavity may be varied through an external adjustment which allows slight rotation of the spherical mirror about an axis perpendicular to both the laser optical axis and the flow direction. In this manner, the streamwise location x_c of the optical axis (co-normal of the mirrors) may be varied across the entire 10-cm diameter of the mirrors. This adjustment permits determination of the optimal co-normal location for given flow conditions, i.e., the location which produces maximum outcoupled power. When coupled with the cavity radiation intensity measurements from the various sampling holes, the adjustment also allows a determination of the spatial extent of the lasing zone for different locations of x_c. Intentional misalignment of the mirror pair through the x_c adjustment results in turn-off of the lasing action. Measurements of mirror temperature rise for operation in this mode decouple the conduction mirror heating due to flow chemistry from mirror heating due to lasing. Such experiments provide a baseline for measurements of mirror heating (outcoupled energy) due to lasing.

Flow and Combustion Measurements

Schlieren motion pictures of the region immediately upstream of the shock holder inlet were obtained for detonable mixtures using both helium and argon as diluents. The photographs were taken in a horizontal view which is that of Figs. 1, 3, and 4. Representative frames from a selected experiment using argron diluent are shown in Fig. 5. The Schlieren measurements were compared with the associated oscillograph record of flow pressures and temperatures. Frame numbers and time are referenced to the time of argon turn-on as evidenced both by the first appearance of a shock pattern and the rise of oscillograph pressure channels. Fluorine turn-on was delayed to show the stable occurrence of a shock which entered the shock holder as shown in Fig. 5a. After fluorine turn-on, combustion was verified by the oscillograph response of gas probe thermocouples and flow

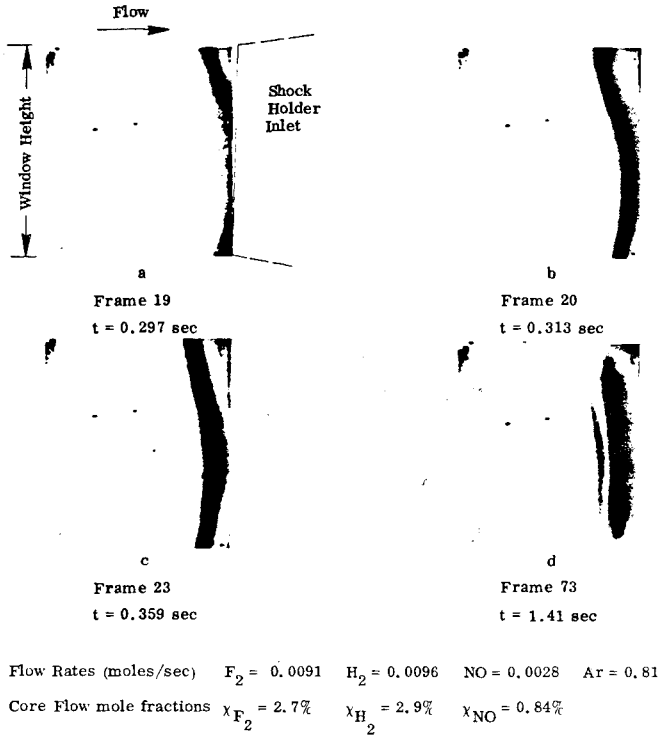

Fig. 5 Schlieren photographs upstream of shock holder entry with detonable gas composition.

pressures. Stable flow was quickly established with combustion, and the shock assumed a new position ahead of the shock holder inlet as shown in Fig. 5b. During the entire period of steady flow, the shock pattern retained the general shape shown in Figs. 5b and 5c, but occasionally showed small oscillations in the flow direction of amplitude ± 3 mm. Steady flow termination occurred at $t = 1.42$ s, when supersonic static pressure indicated the occurrence of shocks in the supersonic mixing section. This pressure increase coincided with the disappearance of a shock wave in the Schlieren photographs. In summary, all flow events indicated by oscillograph pressure and temperature measurements were verified by coincident events in Schlieren photographs, and stable shock formation was established in a detonable mixture with operating conditions given in Fig. 5. Similar Schlieren observations were made visually with detonable mixtures using helium diluent, and with shock entry heights of both 2.51 and 2.11 cm; however, contrast was insufficient to provide convincing photographic records.

An oscillograph record is shown in Fig. 6 for operating conditions listed in Table 2. Channel 1 records each of ten temperatures at intervals of 0.1 s in the sequence nozzle temperature T_n, gas probes T_{g1} through T_{g5}, and mirror thermocouples T_{m_1} through T_{m_4}, as shown. Channel 2 records four pre-orifice supply gas pressures in the sequence $p_r(F_2)$, $p_r(H_2)$, $p_r(NO)$, $p_r(He)$. This cycle is executed twice between each 0.1-s timing mark. Channels 3, 4, 5, and 6 continuously record the primary plenum pressure p_{10}, supersonic static pressure p_{ss}, spill flow pressure p_{sf}, and shock holder pressure p_{sh}, respectively. Channels 7-9 record the cavity radiation intensity signals from the oscillating vertical array of three lead-selenide detectors. Only the center and bottom detector channels, channels 8 and 9 respectively, are shown. The data in channels 8 and 9 and the oscillating arm driver signal in channel 10 are discussed in the next section.

Channel 2 shows the initiation of He and F_2 flows at the right with time increasing to the left; H_2 and NO flow have already reached steady state. Flow pressure channels 3-6 show rapid achievement of steady state which continued for a

Table 2 Operating conditions corresponding to Fig. 6

Flow rates (mole/s)	$F_2 = 0.052$	$H_2 = 0.010$
	$NO = 0.020$	$He = 0.86$
Core flow mole fractions	$\chi_{F_2} = 13.7\%$	$\chi_{H_2} = 2.7\%$
	$\chi_{NO} = 5.4\%$	$\chi_{He} = 78.2\%$
Optical axis(wr.t.inlet)	$x_c = 3.28$ cm	
Inlet height	$= 2.11$cm	
Primary plenum pressure	$p_{10} = 64$ Torr	
Supersonic static pressure	$p_{ss} = 2.4$ Torr	
Spill flow pressure	$p_{sf} = 1.7$ Torr	
Shock holder pressure	$p_{sh} = 13.4$ Torr	

Mirror instrumentation configuration A (see Fig. 4)

Shock holder gas temperatures (positions referenced to shock holder entry)

$x_1 = 1.66$ cm	$\Delta(Tg_1) = 0.0°C$
$x_2 = 3.22$ cm	$\Delta(Tg_2) = 474°C$ (laser radiation heating)
$x_3 = 4.78$ cm	$\Delta(Tg_3) = 245°C$
$x_4 = 6.35$ cm	$\Delta(Tg_4) = 350°C$
$x_5 = 33$ cm	$\Delta(Tg_5) = 360°C$

period of 0.4 s. Subsequently, the spill flow pressure (channel 5) rises slowly while constant pressures are maintained in the primary plenum (channel 3), in the supersonic mixing section (channel 4), and in the shock holder (channel 5). Gas thermocouples 1, 3, and 4 demonstrate combustion in the shock holder with a delay that is associated with their thermal response time. Gas thermocouple 2 in this case is nearly coincident with optical axis position $x_c = 3.28$ cm, and, consequently, shows a strong response to cavity radiation. Gas thermocouple 6, with a gain 0.4 times that of the other gas thermocouples, shows a response representative of complete combustion and mixing within the shock holder of core and shroud flows. A dramatic change in combustion history is apparent approximately 0.9 s after flow initiation. This change is not clearly understood but might be related to slight variations in shock holder flow which result from the observed increase in spill flow pressure. This is nearly coincident with the termination of laser operation as indicated by T_{g2} and i.r. channels 8 and 9 which are discussed in the next section. Table 2 shows a pressure recovery between the supersonic mixing section and the shock holder of $p_{sh}/p_{ss} = 5.6$. Unmixed core flow final temperature rise for the listed composition is 660°C.

Table 3 Shock-holder (laser cavity) pressures and reactant concentrations in laser performance tests

Pressure, Torr	Reactant molar concentration, % F_2	H_2	NO
25	6.5	2.6	2.6, 5.4
13	2.7, 5.8, 13.7	2.7	2.7, 5.4, 11.0
6	13.7	1.3, 2.7	2.7, 5.4

The distribution of total flow between the spill flow and that captured by the shock holder was found to be in the proportions 30% and 70%, respectively. This result was determined by two independent calculations: one was based on measured shock holder stagnation pressure and temperature and the known shock holder throat area; the other was based on the measured rate of increase of spill flow pressure and the known spill flow dump tank volume. If complete mixing of reactive core flow (40% of total flow) and the captured fraction of inert shroud flow (30% of total flow) is assumed at the location of gas probe thermocouple 5, then the predicted temperature rise is 392°C. This calculation compares favorably with the measured value in Table 2.

Laser Measurements

The performance of the shock-initiated laser was evaluated for a range of gas pressures and compositions. Laser instrumentation configuration A was used in the majority of these experiments, with emphasis on measurement of the total outcoupled power. These measurements were based on mirror calorimetry and analyses of local heating using the mirror thermocouple data and were reinforced by the infrared cavity radiation measurements. The run conditions corresponding to maximum observed outcoupled power were then used in a smaller set of experiments with the instrumentation in the B configuration. In these experiments, where finer detail in the cavity intensity measurements was obtained, the extent of the lasing zone in the flow direction and the variation of outcoupled power with mirror co-normal position x_c were determined.

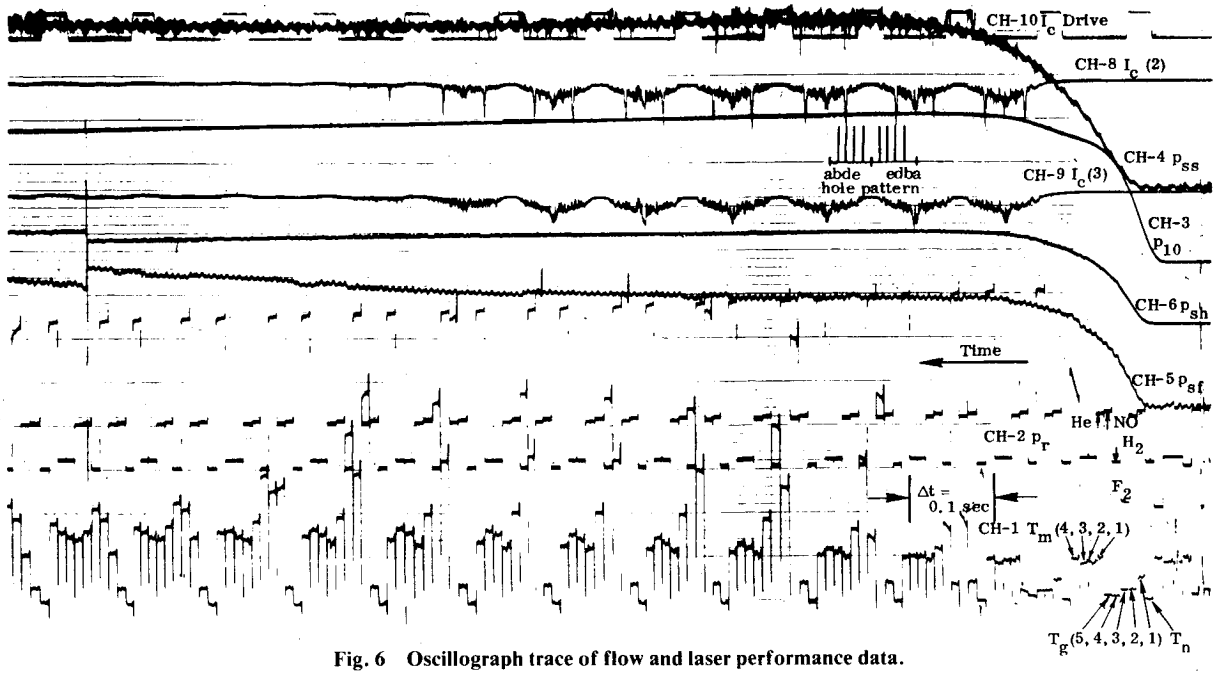

Fig. 6 Oscillograph trace of flow and laser performance data.

Three postshock cavity pressures (approximately 25, 13, and 6 Torr) were used, and several gas mixtures were tested at each pressure with emphasis on variations in the ratio of F_2 to NO concentrations. The NO is intended to initiate the chain reaction by F atom formation; however, the NO concentration might also influence performance of the chain reaction laser through H-atom extinction by FNO or vibrational quenching of HF by FNO or NO. The approximate reactant concentrations used at each of the three pressures are shown in Table 3. Helium diluent was used in all experiments discussed in this section.

Fluorine gas used in some of the laser experiments was analyzed with a quadrupole mass spectrometer. Results indicated that O_2, N_2, and HF were present as impurities, with the O_2 and HF impurities estimated as 1.2 and 3.5%. A cold trap was introduced which utilized acetone cooled to its triple point (178 K) with liquid nitrogen. The trap was used to freeze out HF as the fluorine from the supply bottle passed slowly through the filling system. Comparative experimental runs were made with the shock-initiated laser using the purified and unpurified F_2 sources. The measurements of cavity intensity did not exhibit any significant differences, and estimates of the laser outcoupled power based on mirror calorimetry were inconclusive. These results suggested that improvement of laser performance by F_2 purification was at best marginal, and the F_2 purity studies were not pursued further.

To relate measurements of outcoupled laser power based on mirror calorimetry to estimates based on the direct radiation measurements of cavity intensity, the mirror absorptivity must be known. Absolute measurements of specular mirror reflectivity were made using a pulsed discharge HF laser, operating on transitions in the $v=2\rightarrow1$ and $v=1\rightarrow0$ HF bands. Mirror absorption was estimated from these measurements. The mirrors, mounted in their cavity support/alignment structure, were oriented such that the pulsed laser beam entered at the leading edge of the mirror set and reflected back and forth between the two mirrors (typically 18 times) before re-emerging at the leading edge. The pattern and number of reflections were observed with a coaligned He-Ne laser. The HF laser beam energy was measured before and after the mirror traverse with a fast-response joulemeter. This measured loss in beam energy sets an upper bound on the mirror absorptivity. (Other specular beam losses would be mainly due to nonspecular reflection.)

Measurements on a new set of ThF_4-coated OFHC copper mirrors indicated a reflectivity of 0.97. These mirrors were used in the laser performance experiments using configuration A. After approximately 60 runs, the mirrors were found to be coated with a visible residue and the measured reflectivity dropped to 0.91. A second set of mirrors of slightly different manufacture (used in configuration B) had a measured reflectivity of 0.95 prior to installation. The apparent deterioration of mirror reflectivity with time contributes to uncertainties in those estimates of the outcoupled power which are based on cavity intensity measurements.

One run from the martrix of performance tests is selected for discussion here. This run, designated run 42, with a core flow $F_2/H_2/NO$ composition of 13.7%/2.7%/5.4% at a cavity pressure of 13 Torr, corresponds to the maximum observed cavity intensity. The flow history and gas probe thermocouple data for run 42 are discussed in the previous section, and the operating conditions are summarized in Table 2. The raw data in the form of the oscillograph record are shown in Fig. 6. For the present discussion, the pertinent data channels are channels 8 and 9, which record the cavity radiation signals, and channel 1, which records the thermocouple signals. Channel 10 indicates the lateral position of the oscillating PbSe detector array. The pattern of the cavity-sampling hole positions is indicated by the scale in the figure.

The signal from the middle detector (channel 8) shows a sharp spike in response, corresponding to a location in line with hole b (see Fig. 4). Hole b, at a location 3.28 cm from the mirror leading edge, corresponds to the location of the optical axis (mirror co-normal) for this experiment and would, therefore, be expected to be near the location of maximum cavity intensity. The spike in the detector response is due to the diffracted radiation through sampling hole b. This spike does not appear in the response of the bottom detector (channel 9) which was positioned such that it was outside the diffracted radiation pattern. The hash-like signal which appears in both detectors over much of the traverse is due to extraneous radiation diffracted from the front edge of the mirrors or passed by the off-axis mirror hole (hole f in Fig. 4) which was used for mirror alignment. This extraneous background was greatly reduced in subsequent experiments by the addition of light baffles. No signal above the background is apparent in channel 8 for locations in line with hole a ($x=0.424$ cm) or hole d ($x=6.14$ cm). This result indicates that the lasing zone for this condition is confined to a region less than 5.7 cm long. Further detail relating to the extent of the lasing zone was obtained in experiments using instrumentation configuration B. These experiments are discussed later in this section.

The total outcoupled laser power for the experiment discussed above was calculated using two approaches: mirror calorimetry measurements and estimates based on the cavity intensity measurements. For the mirror calorimetry measurement, the mirror heating is measured by monitoring the total temperature rise indicated by the mirror thermocouples. A steady, uniform (to within ±8% for the six thermocouple pairs) mirror temperature is obtained within 30 s from run initiation. This time is short compared to the characteristic conduction cooling time for the mirror assembly; therefore, the final steady temperature may be taken as a measure of heating due to lasing and conduction from the hot reacting gases. Mirror heating due to lasing may be isolated from conduction heating by measurement of the mirror temperature increase when the mirrors are deliberately misaligned (through the external x_c adjustment) such that no lasing occurs. In the experiment discussed above, the conduction heating measured for the nonlasing case amounted to approximately 65% of the total heating (conduction plus lasing) measured in the lasing case. The energy absorbed by the mirrors due to lasing was inferred to be 41 J, corresponding to a temperature increase of 0.13°C. A lasing duration of 0.75 s was indicated by the cavity radiation data. The outcoupled energy of 41 J is equivalent to an average outcoupled power of 55 W over this duration.

The infrared radiation signal recorded in channel 8 may be directly converted to cavity mirror incident radiation on the basis of the calibration discussed previously. The peak deflections of approximately 1.1 cm in the channel 8 signal correspond to a peak cavity incident intensity of approximately 110 W/cm^2. Estimating the outcoupled power from this measurement requires estimates of the extent of the two-dimensional lasing zone and knowledge of both the

Table 4 Summary of laser performance for run 42 (maximum observed output power)

Composition, %	
He	78.2
F_2	13.7
H_2	2.7
NO	5.4
Cavity pressure	13 Torr
Optical axis (x_c)	3.28 cm
Laser duration	0.75 s
Cavity intensity ($x=3.28$ cm)	110 W/cm^2
Outcoupled power	
Mirror calorimetry	55 W
Cavity radiation	50 W
Chemical efficiency	1%

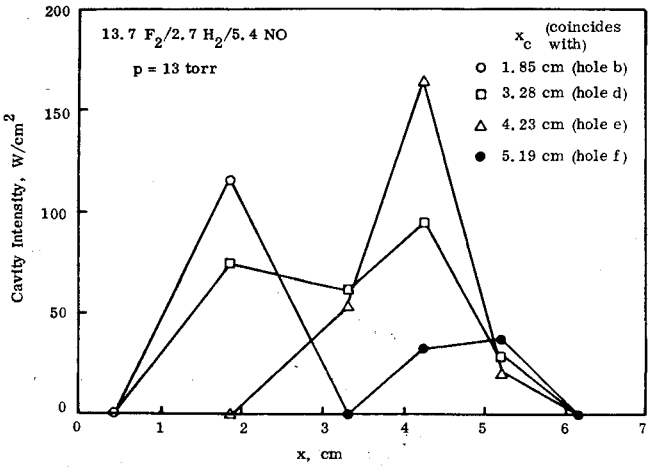

Fig. 7 Measured cavity intensity distributions with variation in optical axis location.

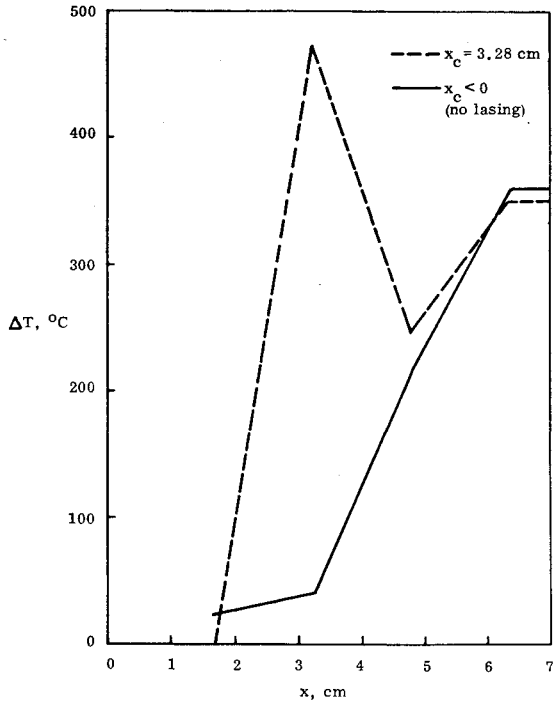

Fig. 8 Measured gas probe thermocouple response for flow conditions of run 42.

spatial distribution of cavity intensity over the lasing zone and of the mirror absorptivity. For an absorptivity of 0.05 and with reasonable assumptions regarding the lasing zone which are based on the flow geometry and the spatial limits inferred from the cavity intensity measurements, an outcoupled power of approximately 50 W is estimated. This estimate is in good agreement with the calorimetry result of 55 W and is also in good agreement with subsequent experiments with the same gas mixture using configuration B.

The chemical efficiency inferred for the composition and flow rates of Table 2 is 0.96%. The laser performance associated with run 42 is summarized in Table 4. Although the chemical efficiency associated with this run was the optimum for the set of experimental conditions considered, this performance may not represent the ultimate potential of the shock-initiated laser system.

Fluid mechanics effects inherent in the present system (viscous effects, flow separation, and shock instabilities), the short single-pass gain path (10 cm), and spillage of cavity radiation off the leading edge at the mirrors are effects which

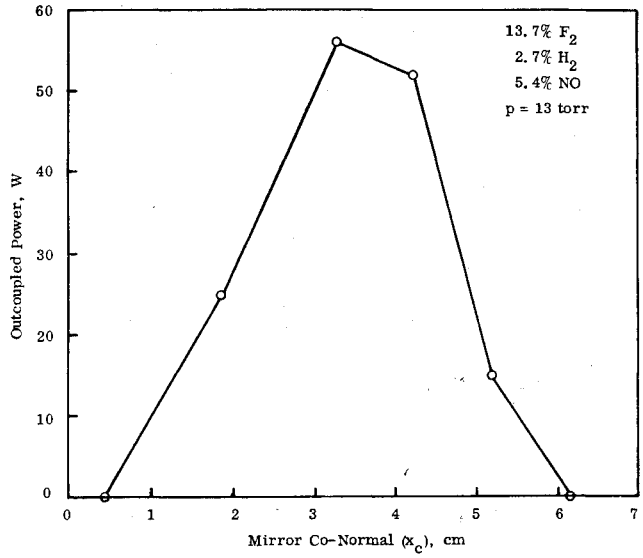

Fig. 9 Variation in outcoupled laser power with optical axis location.

result in reduced performance compared to the potential of a large-scale, shock-initiated laser system.

A series of experiments was conducted with the same flow conditions as run 42 to obtain more detailed information on the spatial extent of the lasing zone, the spatial variation of cavity intensity within the lasing zone, and the variation of total outcoupled power with changes in the optical axis location. These results were obtained with mirror configuration B by varying the position of x_c to coincide with each of the radiation sampling hole locations. This procedure was continued downstream until an optical axis location was reached where no lasing occurred. The results of these experiments are shown in Figs. 7-9.

Figure 7 indicates the measured cavity intensity distributions. The peak cavity intensity is typically $\geq$ 100 W/cm^2 for x_c between 1.8 and 4.2 cm, with the location of peak intensity in general coinciding with the optical axis location. The longest lasing zone was obtained with x_c at 3.28 cm, which corresponds to the optical axis location for maximum power. For this location of x_c, the lasing zone extends from streamwise locations less than 1.85 cm to locations beyond 5.2 cm and is thus at least 3.4 cm in length. No laser emission was observed at $x = 0.424$ cm or $x \geq 6.14$ cm for any position of the optical axis. As indicated by the gas temperature measurements discussed above, the temperature of the reactive gases at $x = 6.35$ cm is approximately 650°C for the gas mixture used in these experiments. At the high downstream temperatures, lasing ceases because the gain of individual laser lines is greatly reduced. This reduction in gain is due to broadening of the rotational distribution as well as depopulation of the excited vibrational levels.

The measured responses of the gas probe thermocouples are plotted in Fig. 8 for run 42 ($x_c = 3.28$ cm) and for the nonlasing case corresponding to the same flow conditions and gas composition. The laser radiation heating of gas probe thermocouple 2 is apparent in this figure.

The results for the total outcoupled laser power are shown in Fig. 9. The magnitude of the power was estimated from the cavity intensity measurements discussed above. The maximum power, with x_c at 3.28 cm, is in good agreement with the power measurements in run 42 using configuration A. A chemical efficiency of 1% for this combination of gas mixture and optics may again be inferred.

Summary

A new kind of chain reaction cw HF laser has been developed. Initiation is by atomic fluorine produced in the reaction $NO + F_2 \rightarrow FNO + F$. Uniform premixing of the

reactant gases is achieved with negligible reactions in a cold supersonic stream, and combustion is initiated by a nearly-normal stationary shock. This work represents the first reported demonstration of cw chemical laser action by stationary shock initiation.

Flow and combustion diagnostics, including Schlieren photographs and gas probe thermocouple measurements, confirmed the achievement of steady combustion initiated by a nearly-normal stationary shock. A closed cavity stable resonator laser configuration was used in the shock holder, and HF laser action was confirmed both by measurements of the i.r. cavity intensity and by mirror calorimetry.

The gas mixture, pressure, and location of the optical axis were varied in a series of laser performance tests. The primary diagnostics were measurement of the total outcoupled laser energy for each run condition, and measurement of the laser cavity intensity with partial spatial and temporal resolution. For this matrix of tests, optimum performance was achieved in a mixture of 13.7% F_2, 2.7% H_2, 5.4% NO, in helium diluent, with a shock holder pressure of 13 Torr. The optical axis (mirror co-normal) was located approximately 3.3 cm downstream from the normal shock. A total outcoupled energy of 41 J over a lasing duration of 0.75 s was measured, corresponding to 55 W average power. A lasing zone at least 3.4 cm long was indicated, with peak cavity intensity of approximately 100 W/cm^2. The chemical efficiency for these conditions was conservatively estimated to be 1%.

The laser performance measured in this study, which is somewhat modest compared with the more fully developed cold reaction laser schemes, may not represent the ultimate potential of the shock-initiated HF laser. Fluid mechanics effects inherent in the present system (viscous effects, flow separation, and shock curvature and instabilities), the short single-pass gain path (10 cm), and spillage of laser radiation from the high-Fresnel number cavity are effects which result in reduced performance.

Acknowledgments

The authors gratefully acknowledge contributions in the chemical and optical aspects of this study from Morton Camac, Charles Kolb, and Fritz Bien of Aerodyne Research, Inc. This work was sponsored by the Navy/Defense Advanced Research Project Agency under Contract N00173-78-C-0011.

References

[1] Kolb, C. E., "Resonance Fluorescence Study of the Gas Phase Reaction Rate of Nitric Oxide with Molecular Fluorine," *Journal of Chemical Physics,* Vol. 64, April 1976, pp. 3087-3090.

[2] Gross, R. W. F., Giedt, R. R., and Jacobs, T. A., "Stimulated Emission Behind Overdriven Detonation Waves in F_2O-H_2 Mixtures," *Journal of Chemical Physics,* Vol. 51, August 1969, p. 1250.

[3] Bowen, J. R., and Overholser, K. A., "An Appraisal of the Continuous Explosion Laser,"*Astronautica Acta,* Vol. 14, 1967, pp. 475-485.

[4] Cool, T. A., Stephens, R., and Shirley, J. A., "HCl, HF, and DF Partially Inverted cw Chemical Lasers," *Journal of Applied Physics,* Vol. 41, Sept. 1970, pp. 4038-4050.

[5] Nicholls, J. A., Dabora, E. K., and Gealer, R. L., "Studies in Connection with Stabilized Gaseous Detonation Waves," *Proceedings of the Seventh Symposium (International) on Combustion,* The Combustion Institute, 1958, pp. 766-772.

[6] Nicholls, J. A. and Dabora, E. K., "Recent Results on Standing Detonation Waves," *Proceedings of the Eighth Symposium (International) on Combustion,* The Combustion Institute, 1960, pp. 644-655.

[7] Nicholls, J. A., "Standing Detonation Waves," *Proceedings of the Ninth Symposium (International) on Combustion,* The Combustion Institute, 1962, pp. 488-498.

[8] Gross, R. A., "Design Report, Supersonic Combustion Tunnel," Air Force Office of Scientific Research Report AFOSR-TN-57-677, Sept. 1957.

[9] Richmond, J. K. and Shreeve, R. P., "Wind-Tunnel Measurements of Ignition Delay Using Shock-Induced Combustion," *AIAA Journal,* Vol. 5, 1967, p. 1717.

[10] Suttrop, F., "Experiments Investigating Shock-Induced Combustion for Applications in Hypersonic Propulsion Engines," VI Europaischer Luftfahrt Kongress, Munchen, Germany, Sept. 1965.